Global Biogeochemical Cycles

RESEARCH ARTICLE
10.1029/2020GB006880

Impact of Lagrangian Sea Surface Temperature Variability on Southern Ocean Phytoplankton Community Growth Rates

Jessica Zaiss[1], Philip W. Boyd[2], Scott C. Doney[3], Jon N. Havenhand[4], and Naomi M. Levine[5]

[1]Department of Earth Science, University of Southern California, Los Angeles, CA, USA, [2]Institute for Marine and Antarctic Studies, University of Tasmania, Hobart, TA, Australia, [3]Department of Environmental Sciences, University of Virginia, Charlottesville, VA, USA, [4]Department of Marine Science, University of Gothenburg, Strömstad, Sweden, [5]Department of Marine and Environmental Biology, University of Southern California, Los Angeles, CA, USA

Key Points:

- Sea surface temperature (SST) variability differs between the Lagrangian and Eulerian reference frames
- SST variability on timescales of days to weeks encountered by advecting phytoplankton decreases phytoplankton community growth rates
- The commonly used Eppley curve or Q_{10} growth models do not capture the effects of SST variability on phytoplankton growth

Supporting Information:

Supporting Information may be found in the online version of this article.

Correspondence to:

N. M. Levine,
n.levine@usc.edu

Citation:

Zaiss, J., Boyd, P. W., Doney, S. C., Havenhand, J. N., & Levine, N. M. (2021). Impact of Lagrangian sea surface temperature variability on Southern Ocean phytoplankton community growth rates. *Global Biogeochemical Cycles*, *35*, e2020GB006880. https://doi.org/10.1029/2020GB006880

Received 4 NOV 2020
Accepted 19 JUL 2021

Abstract Ocean phytoplankton play a critical role in the global carbon cycle, contributing ~50% of global photosynthesis. As planktonic organisms, phytoplankton encounter significant environmental variability as they are advected throughout the ocean. How this variability impacts phytoplankton growth rates and population dynamics remains unclear. Here, we systematically investigated the impact of different rates and magnitudes of sea surface temperature (SST) variability on phytoplankton community growth rates using surface drifter observations from the Southern Ocean (>30°S) and a phenotype-based ecosystem model. Short-term SST variability (<7 days) had a minimal impact on phytoplankton community growth rates. Moderate SST changes of 3–4°C over 7–45 days produced a large time lag between the temperature change and the biological response. The impact of SST variability on community growth rates was nonlinear and a function of the rate and magnitude of change. Additionally, the nature of variability generated in a Lagrangian reference frame (following trajectories of surface water parcels) was larger than that within an Eulerian reference frame (fixed point), which initiated different phytoplankton responses between the two reference frames. Finally, we found that these dynamics were not captured by the Eppley growth model commonly used in global biogeochemical models and resulted in an overestimation of community growth rates, particularly in dynamic, strong frontal regions of the Southern Ocean. This work demonstrates that the timescale for environmental selection (community replacement) is a critical factor in determining community composition and takes a first step towards including the impact of variability and biological response times into biogeochemical models.

Plain Language Summary Ocean phytoplankton are fundamental to the global carbon cycle. However, it remains unclear how environmental variability impacts phytoplankton growth, and thus, the global carbon cycle. Phytoplankton encounter environmental variability (e.g., sea surface temperature [SST] changes) as they are transported throughout the oceans by surface currents. Here, we quantified this variability (i.e., in a Lagrangian reference frame) using surface drifters and investigated the impact of this variability on phytoplankton community growth rates using an ecosystem model. We also compared the Lagrangian SST to the SST variability of a fixed point (e.g., a buoy) where ocean currents flow past (i.e., the Eulerian reference frame) using high-resolution satellite data. We found larger SST changes in the Lagrangian than in the Eulerian reference frame and discovered that this difference impacted phytoplankton community structure and growth rates. The impact of SST variability was not captured by the growth model that is typically used by global biogeochemical models. Our results provide an important extension on the classic principle that "everything is everywhere: but the environment selects" (Hutchinson, 1961, https://doi.org/10.1086/282171). Even when "everything is everywhere", we show that the timescale for environmental selection (community replacement) is a critical factor in determining community composition.

1. Introduction

Phytoplankton are a fundamental part of the global carbon cycle accounting for nearly 50% of all photosynthesis globally (Falkowski et al., 2008). Phytoplankton also serve as the base of the marine food web and

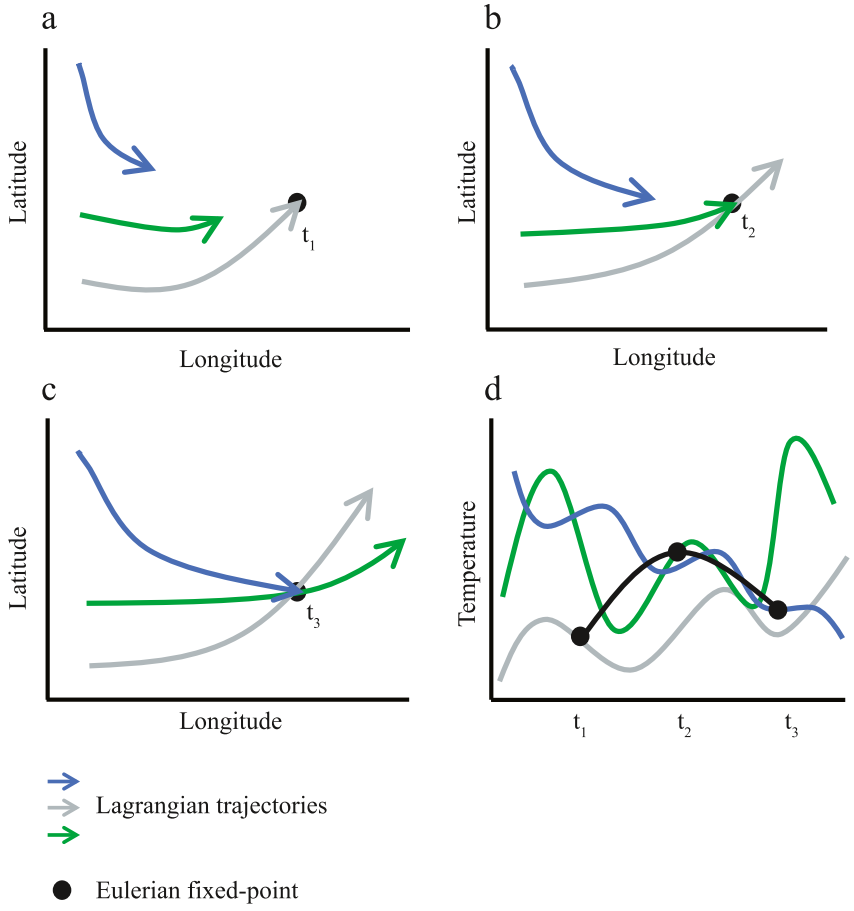

Figure 1. Lagrangian versus Eulerian reference frames. Lagrangian reference frames follow the water parcel itself through time. The Eulerian reference frame refers to a fixed point in space (e.g., buoys or mooring stations) where advection of water parcels floating past the fixed point generates temporal variability. Panels (a–c) depict three different water masses (gray, blue, and green) as they each pass through the fixed Eulerian location (black dot) at times t_1, t_2, and t_3. Panel (d) shows the temperature of each water mass through time (gray, blue, and green lines) as well as the temperature recorded at the Eulerian location (black line). Note in panel (d) that overall temperature variability in the Lagrangian reference frame (gray, blue, and green lines) is much greater than that in the Eulerian reference frame (black dots) though this may not always be the case.

drive the ocean biological carbon pump, which acts to sequester carbon in the deep ocean. Understanding the impact of rising global temperatures on phytoplankton communities is therefore critical for predicting the influence of anthropogenic warming on ocean ecosystems and the global carbon cycle (Doney, 1999; Quéré et al., 2005). Currently, the parameterization of temperature-dependent growth rates is one of the main sources of uncertainty for future carbon cycle predictions among global biogeochemical models (Laufkötter et al., 2015). Due to their planktonic nature, phytoplankton will encounter anthropogenic warming in two ways: (a) as a general warming overlain on top of significant temperature variability due to advection; and (b) as changes in variability driven by large-scale shifts in ocean physics (Boyd et al., 2016; Fu et al., 2016; Lomas et al., 2010). Both of these processes will shift the type and magnitude of temperature variability experienced by phytoplankton. Therefore, an improved understanding of the impact of temperature variability on phytoplankton growth rates is necessary in order to mechanistically incorporate phytoplankton growth dynamics into biogeochemical ecosystem models and to generate robust predictions of future changes.

Accurately assessing the type of temperature variability (rate and magnitude of change) encountered by phytoplankton in the ocean requires the correct reference frame. For phytoplankton, the correct reference frame is Lagrangian (along trajectory) rather than an Eulerian (fixed location) reference frame (Figure 1).

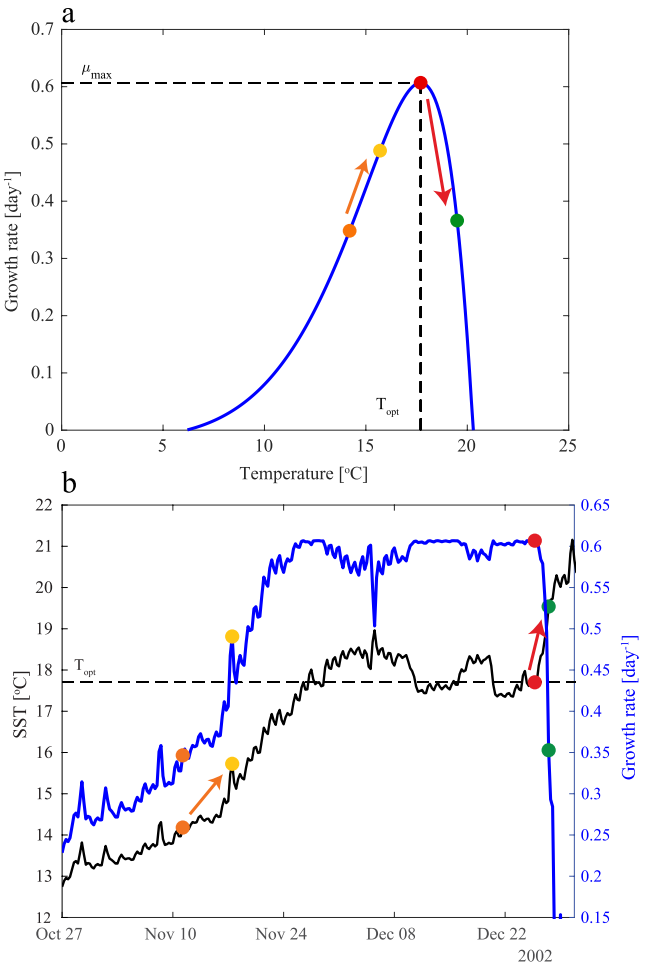

Figure 2. The impact of sea surface temperature (SST) variability on individual phenotype growth rate. (a) The temperature related growth response for a phenotype with a skewed shaped reaction norm. The values for the optimum growth temperature (T_{opt}) and the corresponding maximum growth rate (μ_{max}) are shown with dashed lines. (b) The 90-day SST profile of an example drifter trajectory (black) and the associated changes in phenotype growth rate (blue). The orange and red arrows in the top panel indicate the change in the phenotype growth rate associated with the corresponding changes in SST in the bottom panel.

Modeling studies have demonstrated that both mean conditions and variability (magnitude and rate of change) can differ markedly between the two reference frames (e.g., Doblin & van Sebille, 2016). Here we quantify the nature of the variability experienced by phytoplankton along Lagrangian trajectories using *in situ* data from the Southern Ocean—a region where global climate models lack a consensus on the impact of anthropogenic warming on phytoplankton growth (Bopp et al., 2013). This analysis allows us to constrain realistic rates and magnitudes of temperature changes experienced by Southern Ocean communities and to determine the impact of this variability on population growth rates.

The response of a phytoplankton community to changes in temperature is driven by individual phytoplankter dynamics. Growth rate as a function of temperature (reaction norm) for an individual phytoplankter is unimodal and tends to be asymmetric, often with a skewed tail towards lower temperatures (Boyd, 2019). Therefore, the growth response for an individual phytoplankter to a change in sea surface temperature (SST) depends on the starting SST relative to the optimum growth temperature (T_{opt}, the temperature with the highest growth rate) and whether the SST change is increasing or decreasing (Figure 2). The rate of change in growth rate will depend on the acclimation rate (how fast the phytoplankter adjusts to the new temperature) and type of acclimation of the phytoplankter (Kremer et al., 2018). When SST changes are slower than the phytoplankter acclimation rate, the instantaneous growth rate will be equivalent to the acclimated growth rate (i.e., the phytoplankter is able to keep up with the rate of temperature change). When the rate of SST change is faster than the rate of acclimation, the instantaneous growth rates could be higher or lower than the acclimated growth rate, depending on the type of response, detrimental or beneficial, respectively (Kremer et al., 2018).

Laboratory based experiments on the impact of temperature variability on phytoplankton growth have produced conflicting results. Some studies found an overall decrease in growth rates in a thermally variable environment relative to a stable environment (Bernhardt et al., 2018; Qu et al., 2019; Wang et al., 2019), while others found higher growth rates under variable conditions (Schaum et al., 2018), and some found that thermal variability did not impact community growth rates (Kling et al., 2019; Qu et al., 2019). The lack of consensus concerning the impact of variability on phytoplankton growth rates may be due to the different magnitudes and rates of change used by the different studies, which ranged from ~1.5°C/day (Schaum et al., 2018) to as high as 10°C/day (Bernhardt et al., 2018).

Understanding how an *in situ* population of phytoplankton will respond to temperature fluctuations is further complicated by phenotype and strain diversity. Multiple phenotypes can co-occur within a population of phytoplankton each with different optimal temperatures (T_{opt}, e.g., Webb et al., 2009). As such, the temperature response of a population is often modeled using an Eppley curve (αe^{bT}, Eppley, 1972) where growth rate increases exponentially with temperature rather than as a unimodal relationship (Bopp et al., 2013). In essence, this assumes rapid phenotypic shifts within the community such that, as the temperature changes, the community rapidly shifts its optimal growth temperature (Figure 3b). Previous work has demonstrated that representing phytoplankton growth using an Eppley curve results in an over-estimation of phytoplankton community growth rates (Moisan et al., 2002). In addition, the advection of communities across large temperature gradients, such as those along a western boundary current, can result in considerable differences between the optimum growth temperature (T_{opt}) for the community and the *in situ*

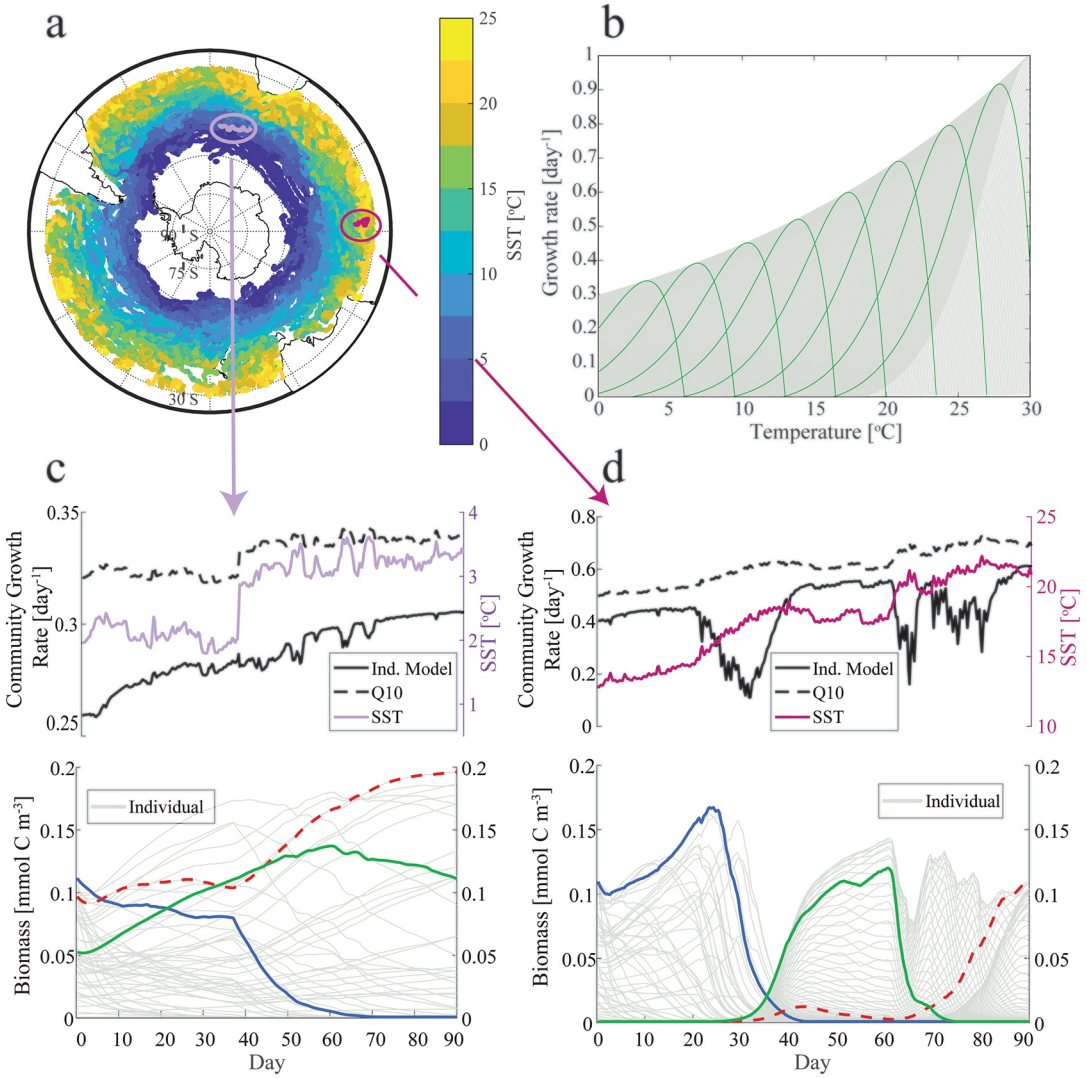

Figure 3. (a) Map of all 90-day drifter trajectories (n = 2,190) colored by sea surface temperature (SST). Two example trajectories are highlighted in purple and magenta. (b) Reaction norms for each of the 319 phenotypes in the ecosystem model. The gray lines represent all the phenotype reaction norms and the green lines are example phenotypes to highlight the reaction norm shape. (c and d) Example trajectories and their resulting model outputs. The top panels show the SST (colors), the community growth rate estimated using the Eppley curve (dashed line), and the community growth rate from our phenotype-based model as calculated using Equation 5 (solid line). The bottom panel shows the biomass through time of each phenotype (gray lines). The blue line follows the phenotype with the highest initial biomass, the red dashed line follows the phenotype that has the highest biomass at the end of the 90 days, and the green line follows the phenotype that has a T_{opt} equal to the mean SST of the trajectory.

temperature (Hellweger et al., 2016). Here we build upon these studies and use a model to assess phenotypic shifts within a population in response to different types of temperature fluctuations and the resulting impact on population (or community) level growth rates.

In this study, we systematically assessed the effect of different magnitudes and rates of change of temperature on phytoplankton community growth rates in the Southern Ocean (south of 30°S) using *in situ* SST data and a numerical ecosystem model. This southern hemisphere region encompasses some of the lowest (0.2°C) and highest (1.6–2.0°C) long-term mean SST variability globally (Deser et al., 2010; Maheshwari et al., 2013). We found that relatively small changes (<2°C over 7–90 days) did not substantially impact community growth rates and that moderate changes (3–4°C over 7–45 days) had the largest and longest lasting effect on community growth rates. These moderate changes resulted in a temporary decrease in community growth rate, that lasted up to 20 generations, as the community responded to the new temperature. The response of community growth rate to variable temperatures was non-linear and so could not easily

be accounted for with an adjustment to the Eppley curve. Finally, we found that the impact of temperature variability on phytoplankton community growth rates was present everywhere in Southern Ocean with the largest impact occurring in regions dominated by meso- and sub-mesoscale activity.

2. Methods

The impact of SST variability on phytoplankton community growth rates was studied by combining SST observations, both *in situ* and from remote sensing products, and a phenotype-based ecosystem model. Here, we focused on the impact of mixed layer SST variability on phytoplankton community growth rates and therefore did not consider growth limitations due to other sources of variability such as nutrients, light, and mixed layer depth (e.g., Rohr et al., 2020a, 2020b). We tested the impact of co-limitation by temperature and nitrate and found that the results were generally consistent with the findings presented here (Text S6). Further work is needed to investigate the impact of multiple un-correlated environmental drivers.

2.1. Southern Ocean Drifter Profiles

Lagrangian SST data were obtained from 422 Southern Ocean surface drifters from the Global Drifter Program with 6-hourly SST data. Float data south of 30°S from July 1999 to April 2016 was downloaded from the Drifter Data Centre at the Atlantic Oceanographic and Meteorological Laboratory (accessed 11/2018). The lifetime of the drifters ranged from 91 days to 5.8 years with a median duration of 521 days. Each drifter was segmented into 90-day trajectories to provide consistency in the data set. We used only segments that had less than 10% of missing data. This resulted in 2,190 90-day trajectories (Figure 3a).

To estimate the magnitude of Lagrangian variability in our study region, we calculated the range of SSTs (ΔSST_{max}) and the time (Δt_{max}) over which the temperature change occurred using moving windows of 1–90 days (in 1-day increments). We then assessed the distribution of variability across different window sizes by aggregating the data into 1°C bins for ΔSST_{max} and 1 day Δt_{max} bins. For example, a 2.4°C change that occurred over 14 days was recorded in the 2–3°C and 14-day bin. To investigate the potential impact of small-scale noise, we also created smoothed splines of each of the 90-day SST profiles using a cubic smoothing spline (*csaps* in Matlab with a smoothing parameter of 0.00001). The splines filter out 25% of the variability on a 1-day timescale up to 95% at the 90-day window (Figure S1). We then repeated the ΔSST_{max} and Δt_{max} analysis on the spline data.

2.2. Remote Sensing SST

To compare the SST variability in the Lagrangian reference frame to the variability that would be captured in the Eulerian reference frame, we used high-resolution (0.01° horizontal resolution and 1-day temporal resolution) satellite SST data from GHRSST Level 4 MUR Global Foundation Sea Surface Temperature Analysis (v4.1) (JPL MUR MEaSUREs Project, 2015; accessed October 2018). This data set spanned 2003–2014 which overlaps with 71% of our 90-day drifter segments. For each 90-day drifter segment between 2003 and 2014, we extracted 90 days of satellite SST data for the latitude and longitude of the final location of the drifter, where the 90 days corresponded to the dates of the drifter segment. We then also extracted the satellite SST along the drifter trajectories to provide a direct comparison between the Eulerian and Lagrangian reference frames in terms of the temporal and spatial resolution of the datasets. We performed the same ΔSST_{max} and Δt_{max} variability analyses for the satellite data as the surface drifter trajectories (described in Section 2.1).

2.3. Idealized SST Trajectories

We complemented the observed SST trajectories with idealized SST trajectories to mechanistically understand the impact of the rate and magnitude of SST change on community growth rates. Specifically, a suite of trajectories ($N = 64$) was generated with both increasing and decreasing SST trends ranging from $\Delta SST = 2°$ to $\Delta SST = 9°C$ (in increments of 1°C) over 7, 21, 45, and 90 days. These ΔSST values and durations were chosen based on our Lagrangian variability analysis. To minimize initialization bias, SST was held constant for the first 30 days before increasing/decreasing. After the SST change, the SST was again held constant until the 200th day. The final temperature for all idealized trajectories was 15°C. The impact

of the final temperature on the model results was analyzed with a set of sensitivity experiments. The final SST had no significant impact on the results when the results were reported in terms of the doubling time (generation), rather than absolute days as this normalized the effect of higher growth rates at warmer temperatures (Text S1). Generation time was calculated as $\ln 2 / \mu_{SS}$, where μ_{SS} is the stabilized community growth rate. With a final SST of 15°C, the generation time was ~1.37 days.

2.4. Phenotype-Based Ecosystem Model

To estimate the impact of variable temperature on phytoplankton community growth rates, we used a phenotype-based ecosystem model. The model consisted of 319 phytoplankton phenotypes that were identical in all aspects (i.e., model parameters) other than the optimal growth temperature (T_{opt}). Temperature dependent growth rate (μ, day^{-1}) was defined as a function of T (°C) (Thomas et al., 2012):

$$\mu(T) = ae^{bT}\left[1 - \left(\frac{T - T_{opt}}{w / 2}\right)^2\right] \quad (1)$$

where T_{opt} was the optimal growth temperature. The value of b controlled the shape of the reaction norm, a (day^{-1}) scaled the reaction norm, and w (°C) defined the width of the reaction norm (the difference between the maximum [T_{max}] and minimum [T_{min}] growth temperatures). We ran the model with two sets of reaction norms: a symmetrical, or broad, curve where $b = 0$ (°C^{-1}) and a skewed reaction norm where $b = 0.3$ (°C^{-1}). Both reaction norms had a width of 14°C ($w = 20$°C), consistent with observed reaction norms for many polar species (Boyd, 2019). Sensitivity tests were performed with reaction norm widths of 10.5°C ($w = 15$°C) and 20.5°C ($w = 29$°C) (Text S2). The results from these sensitivity tests did not differ substantially from the simulations with a reaction norm width of 14°C.

The parameter a scaled the reaction norms at T_{opt} to the Eppley curve (Eppley, 1972) where maximum growth rates ranged between 0.28 day^{-1} at −1.8°C to 1.0 day^{-1} at 30°C, consistent with experimental data (Boyd, 2019). Specifically, a_i was defined for each phenotype i as:

$$a_i = 0.2963e^{0.0405T_{opt}} \quad (2)$$

This resulted in an increase of ~1.5x in growth rate for every 10 degrees (i.e., a Q_{10} relationship of 1.5, *see Discussion*). We generated 319 phenotype curves for both the broad and skewed reaction norms with T_{opt} ranging from −1.8°C to 30°C increasing by 0.1°C (Figure 3b).

The biomass of each phytoplankton phenotype P_i was calculated at each time-step as the integral of:

$$\frac{dP_i}{dt} = \mu_i(T)P_i - m(T)P_i^2 \quad (3)$$

where $\mu_i(T)$ was the temperature-dependent growth rate for phenotype i from Equation 1. $m(T)$ was the temperature-dependent quadratic mortality rate (m^3 mmol C^{-1} day^{-1}) where:

$$m(T) = 0.35 * a \quad (4)$$

Here we used the same temperature dependent Eppley curve (Equation 2) to scale mortality with temperature using SST instead of T_{opt} where $a = 1$ day^{-1} for SST = 30°C. We imposed a minimum biomass (0.001 mmol C m^{-3}) so that no phenotype went locally extinct, akin to the "everything is everywhere" principle (Hutchinson, 1961). Sensitivity tests were performed with the minimum biomass set to 0.0001 mmol C m^{-3}. The minimum biomass threshold did not affect the overall patterns but did increase both the magnitude of the difference from the community growth rates obtained using the Eppley growth model and the time to acclimation (memory length, Section 3.2) for both broad and skewed reaction norms (Text S3). Imposing this minimum biomass purposefully introduced mass into the system which was accounted for by adjusting the biomass of each phenotype to keep the total community biomass at the concentration it would have been without the minimum biomass criteria. Specifically, the total change in biomass without the minimum biomass phenotypes was calculated using the biomass weighted community growth rate (λ) in place of μ(T) in Equation 3, where λ was defined as:

$$\lambda = \sum \mu_{i,t} \frac{P_{i,t}}{P} \quad (5)$$

where, $\mu_{i,t}$ was the growth rate of the *ith* phenotype at time *t* for all phenotypes with biomass greater than the minimum, $P_{i,t}$ was the biomass of the *ith* phenotype whose biomass was greater than the minimum at time *t*, *P* was the sum of the biomass of all phenotypes with biomass greater than the minimum at time *t*.

Several different models for mortality and grazing were tested including linear mortality, constant mortality, a dynamic zooplankton population, and a simple ecosystem model with constant grazing pressure (see Text S4). All model versions resulted in qualitatively similar results which demonstrated that the community dynamics were not particularly sensitive to the top-down control formulation in the model (Text S4). Here, we present the quadratic mortality as it was the simplest model with smooth (non-oscillatory) solutions.

The ecosystem model was forced with each of the 2,190 drifter segments (see Figure 3c & 3d for examples), the corresponding smoothed splines, the idealized SST trajectories, and the satellite-derived SSTs. The initial biomass of phenotypes with a T_{opt} within ±2.5°C of the starting SST value were randomized to simulate previously accumulated biomass with phenotypes outside this range set to the minimum biomass. Simulations that used idealized SST trajectories were performed 100 times with different initial biomass conditions to account for stochasticity in the model initialization.

2.5. Acclimation Rate

To test the impact of different acclimation timescales, we performed sensitivity tests in which we incorporated a linear acclimation rate for all phenotypes in the model. Specifically, we incorporated a timescale over which an individual phenotype could change its growth rate in response to a temperature change. For example, if SST rapidly changed from 15°C to 16°C, a phenotype with an acclimation timescale of 0.2°C day^{-1} would move from the growth rate at 15°C to the growth rate at 15.2°C in one day. If the SST then held constant at 16°C, the phenotype would acclimate by the end of the fifth day. We tested acclimation rates ranging from 0.2°C day^{-1} to 0.6°C day^{-1} in increments of 0.1°C day^{-1} which are consistent with acclimation rates determined for the Southern Ocean diatom *Fragilariopsis cylindrus* (see Table S2). The model with acclimation was forced with the idealized SST trajectories for a ΔSST = 2°C in 7 days (0.29°C day^{-1}), 3°C in 7 days (0.43°C day^{-1}), 4°C in 7 days (0.57°C day^{-1}) and 5°C in 21 days (0.24°C day^{-1}). These intervals corresponded to the magnitudes and rates of change most commonly experienced by the drifter trajectories (see Section 3.1) for which the rate of change was greater than 0.2°C day^{-1}.

3. Results

3.1. SST Variability

We characterized *in situ* SST variability experienced by phytoplankton (i.e., in a Lagrangian reference frame) using the surface drifter SST data. Seasonal dynamics were not filtered out as they were important sources of SST variability encountered by phytoplankton. While the surface drifters may have been subjected to some physical movements that phytoplankton do not encounter (e.g., lateral transfer across fronts due to wind rather than subduction and mixing), they provided the best *in situ* data set for studying Lagrangian variability in surface temperature. However, to minimize the impact of unrealistic fluctuations in the drifter data set, we limited our subsequent analyses to the most frequently measured scales of variability within the drifter record. The average ΔSST_{max} values ranged from 0.9°C ± 0.7°C (1σ) for the 7-day window, which corresponded to 0.13°C/day change over the 7 days, to 4.2°C ± 2.0°C (1σ) for the 90-day window or 0.05°C/day change (Figure S12, Table S1). The latter was consistent with the expected seasonal SST cycle for the Southern Ocean (Reynolds & Smith, 1994). The SST variability of the drifters (standard deviation over the window) was highly correlated with ΔSST_{max} ($R^2 = 0.92$, $p < 0.01$, Figure S13).

Using the ΔSST_{max} analysis, we were able to quantify the most common types of variability encountered *in situ* in terms of both the magnitude of change and the rate of change (Figure 4). Due to the difference in the number of data points generated by the moving windows, we assessed the frequency of each ΔSST_{max} within a given window length (*y*-axis) such that the highest value across the row indicates the most likely ΔSST_{max}

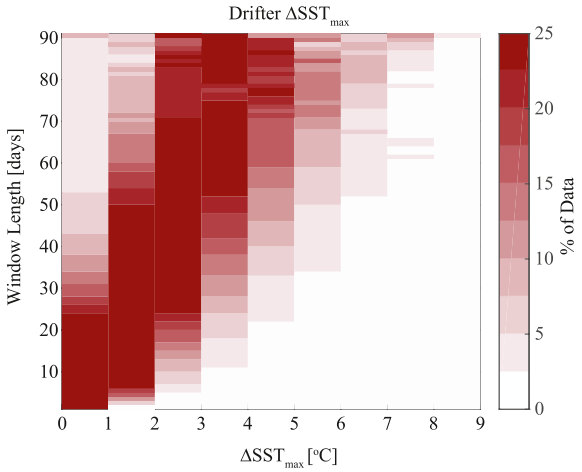

Figure 4. Sea surface temperature (SST) variability analysis. The frequency of ΔSST_{max} changes from the drifter segments over different window lengths are shown. Data are presented as total percent of data that fall within that window length such that each row sums to 100%. There is a general pattern of increasing magnitudes of ΔSST_{max} over longer window lengths.

for that window length. The ΔSST_{max} bins sum to 100% across the row. Overall, there is a trend of increasing ΔSST_{max} with increasing window length, as expected. We selected four representative window lengths, 7, 21, 45, and 90 days, as illustrative examples though the results are not dependent on these selections. A 7-day window was most likely to have a ΔSST_{max} of 2°C or less (82%), and ~3% of the trajectories recorded a ΔSST_{max} of 4°C. Over a 21-day window, most trajectories had a ΔSST_{max} of 2–3°C (combined accounting for 86% of data) and ~10% of the trajectories had a ΔSST_{max} of 4–5°C. ΔSST_{max} reached as high as 9°C for the 90-day windows but accounted for only 2.5% of the data in that window.

A comparison of Lagrangian and Eulerian reference frames demonstrated that, while the overall patterns of variability were similar, the Lagrangian reference frame was more likely to capture large ΔSST_{max} (Figure S14). This was true for both the drifter and satellite derived Lagrangian trajectories when compared to the satellite SST in the Eulerian reference frame. For example, within a time-frame of 21–30 days, a ΔSST_{max} greater than 3°C was more likely to occur in both the drifter and satellite derived Lagrangian (17%) trajectories than in the Eulerian (11%). Similarly, for the 51-day to 60-day windows, ΔSST_{max} of 2–4°C were common in both reference frames, but changes >4°C were more common in the satellite derived Lagrangian trajectories (24%) and the drifter Lagrangian trajectories (23%) than the satellite Eulerian data (16%). This same pattern was consistently observed for all windows from 1 to 90 days. The impact of these differences in SST changes on phytoplankton community growth rates are discussed below (see Sections 3.2 and 3.3).

For most of the SST data recorded by the drifters, the rate of SST change was slower than the expected phytoplankton acclimation rates. Acclimation rates for the Southern Ocean diatom *F. cylindrus* are on average 0.3°C/day (Table S2). For the drifter trajectories, only 8% of the 1-day bins (n = 197,100 days) recorded rates of SST change greater than 0.3°C/day and less than 2% of the daily bins recorded rates of change greater than 0.6°C/day (Figure S15). Because SST rates of change were typically slower than the phytoplankton acclimation rate, we hypothesize that, for the majority of the Southern Ocean, the rate of acclimation will not play a major role in the community response. Therefore, to simplify model dynamics, we ran our model with rapid acclimation such that each phenotype responded directly to SST changes. See Section 4.1 for discussion about situations in which acclimation may be important.

3.2. Impact of Variable SSTs on Community Growth Rates

We used idealized simulations to develop a mechanistic understanding of how variability impacts community growth rates. For small, gradual SST changes of less than 2–3°C in 45–90 days (0.02–0.07°C/day), the community growth rates changed linearly with the SST changes during the period of SST transition and then stabilized once SST stopped changing. When the rate of change was slow, the distribution of phenotypes within the community changed at the same rate as the SST such that the T_{opt} of the most dominate phenotype closely matched the SST. As a result, the temporal response in the community growth rate from the phenotype model was similar to the growth rate from a null model using an Eppley curve parameterization.

For SST rates of change larger than 2–3°C in 45–90 days (0.02–0.07°C/day), community growth rates initially increased or decreased depending on the sign of the SST change, but then began to decrease rapidly (see Figure S16 for example). Once SSTs stabilized at the final value, community growth rates increased and eventually stabilized. Out of the environmentally relevant rates of SST change, 4°C in 7 days (0.57°C/day) resulted in the largest change 70% ± 1% (1σ) during the low growth period (Figure 5a). While the absolute percent change in growth rate was sensitive to model formulation and parameter values, the qualitative relationships presented here were robust (Figure S8).

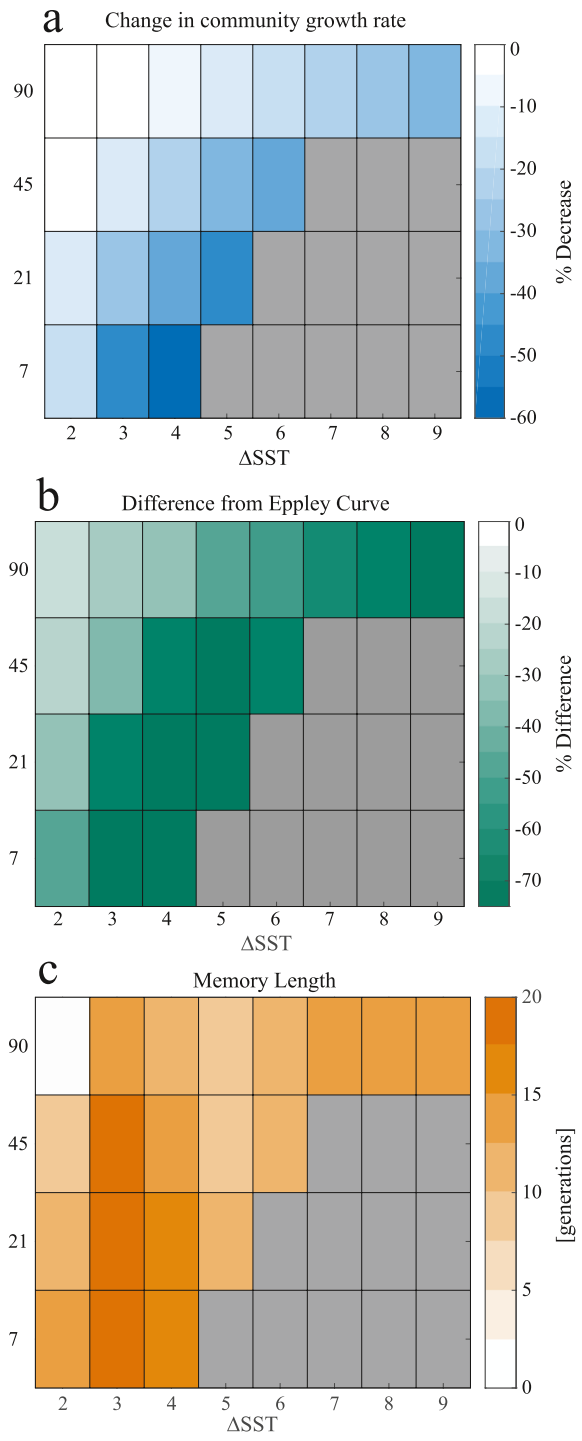

Figure 5. Simulated response of a phytoplankton community with skewed shaped reaction norm to increasing ΔSST (see supporting information for decreasing ΔSST conditions and broad reaction norm results). Panel (a) plots the decline in community growth rate in the phenotype model that results from the sea surface temperature (SST) moving out of the thermal niche of the original population (see Methods and Figure S16). Data that are grayed out represent ΔSST and window length combinations that were not supported by the results from Figure 4. Panel (b) shows the percent difference between the Eppley growth model approximation and the phenotype modeled community growth rates at the point where SST stabilizes (see Figure S16 for example). Panel (c) plots the memory effect length associated with SST changes in the idealized simulations. This represents the time it takes for the community growth rate to be within 5% of the steady state growth rate at the final SST from the first time-step that SST is constant (see Figure S16 for example).

The impact of temperature variability on community growth rates is a function of both changes in the growth rates of individual phenotypes (i.e., shifts along a reaction norm) and shifts in the community composition (i.e., abundance of different phenotypes). The low growth phase after a shift in SST (either increasing or decreasing) was caused by the SSTs extending beyond the thermal optimum of the initial community such that the bulk of the biomass was growing slowly. During this period, the individual phenotypes with elevated growth rates only made up a small fraction of the community and so did not contribute significantly to the community growth rate. The community growth rates then rebounded as these high growth phenotypes increased their biomass and eventually became the dominate biomass group. Faster rates of SST change moved the community out of the thermal optimum of the initial community more quickly than smaller rates of change, and therefore larger and faster ΔSSTs resulted in greater decreases in community growth rates. However, the high growth individuals were able to dominate the community more quickly due to the high loss rates for the slow (or no) growth individuals and so the community growth rates rebounded more quickly for rapid relative to moderate rates of SST change. For rapid SST changes, the rate and type of acclimation response could potentially play a role in the shifts in community growth rates depending on the nature of the plastic response (see *Discussion*).

An Eppley curve was unable to capture the impact of variability in SST on community growth rates due to the non-linear phenotype dynamics. Community growth rates derived directly using the Eppley curve model were always larger than those simulated by the phenotype model, consistent with previous work (Bernhardt et al., 2018; Moisan et al., 2002). The difference between the phenotype modeled growth rates and the Eppley curve estimates varied as a function of SST variability (Figures 5b and S18). As the ΔSST increased over a given window length, so did the difference between the phenotype model and the Eppley curve estimate. The largest departures occurred for ΔSSTs of 4°C and 5°C over 7 and 21 days, respectively, with up to 80% lower simulated community growth rates for the phenotype model. Generally, larger ΔSSTs and faster rates of change (changes occurring over a few generations) resulted in larger differences between the models.

Although we focus on the impact of temperature-limitation on phytoplankton growth in this study, nutrient limitation also plays an important role in co-limiting phytoplankton growth in the Southern Ocean (Cochlan, 2008). While a full analysis of the impact of fluctuating co-limitation is beyond the scope of this study, we conducted a set of model simulations to test the impact of temperature and nitrate limitation on the observed dynamics (Text S6). Given the non-linear formulation of nutrient limitation and the relatively low half-saturation values for the uptake of nitrate, for the majority of the Southern Ocean the model results with co-limitation are similar to those from simulations with temperature limitation only. This is because the variation in nutrient limitation was small compared to the variation in temperature limitation (at the level of individual phenotypes).

3.3. Memory Effect

The timescales of the biological response to temperature fluctuations varied as a function of the overall magnitude and direction (increasing or decreasing) of SST change, the duration of the SST change, and shape of the reaction norm (broad vs. skewed) for the individuals within the population. Here we define the timescale of biological response as the "memory effect"—the time for the community growth rate to stabilize (±5% of the stable value). Here we present the memory effect in terms of generations calculated using the final stable growth rate. This allowed us to understand the relative impact of temperature change on phytoplankton using a common currency such that our results are not growth rate dependent.

The most common ΔSST changes (Figure 4) were associated with the longest memory effects (Figures 5b and S19). Nearly all of the environmentally relevant ΔSST values were sufficient to create a memory effect of longer than two generations. Moderate changes of 3–4°C over 7–45 days or 4–28 generations (0.07–0.57°C/day) resulted in the longest memory effects of up to up to 22 generations for both reaction norm shapes (Figures 5c and S19). This biological response time is nearly 5 times longer than the duration of the temperature change. Larger SST changes (5–6°C) that occurred over 45 or 90 days or 28–57 generations (0.06–0.13°C/day) tended to have shorter memory effects (~8–19 generations) than moderate changes that occurred over the same time frame, but this difference was not statistically significant. Longer memory effects for moderate SST changes resulted from dominant phenotypes in the previously acclimated community being able

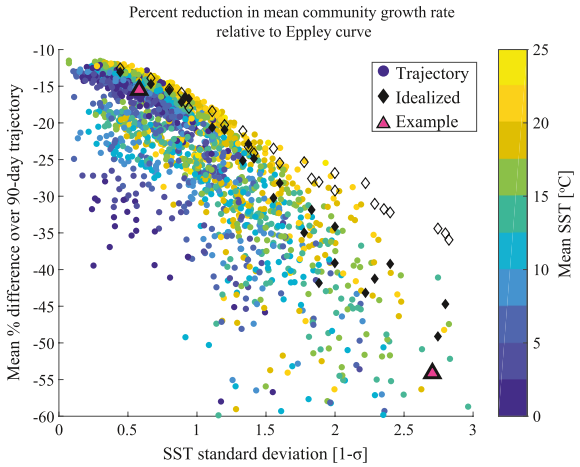

Figure 6. Impact of sea surface temperature (SST) variability on community growth rate. The average percent difference in community growth rate between the phenotype model and the Eppley growth model from the 90-day drifter segments are plotted against the standard deviation (1σ) of the drifter SST. Each segment is colored by the mean SST. Results from the idealized trajectories are shown as black diamonds with filled diamonds denoting increasing SST trajectories and open diamonds denoting decreasing SSTs. Pink triangles represent the two example trajectories from Figure 3. Results shown here are for skewed shaped reaction norms, see Figure S20 for results for the broad shaped reaction norms.

to grow in the new environment, albeit at a reduced rate. This increased the time required for the phenotypes optimally suited for the new environment to dominate the community, which resulted in larger memory effects.

The sign of the SST change also impacted the response time of the community. Decreasing ΔSSTs had longer memory effects by an average of 7 generations compared to increasing ΔSSTs (*t*-test, 95% CI) for the skewed shaped reaction norms. The longer memory effect was due to the long tail on the decreasing side of the reaction norm, which allowed the phenotypes in the initial community to grow during decreasing SST conditions (Figure S19). For reaction norms that were symmetrical about the optimum growth temperature, the direction of ΔSST did not matter, and the memory lengths were not statistically different for increasing and decreasing ΔSSTs (*t*-test, 95% CI) (Figure S19).

3.4. Southern Ocean Drifter Trajectories

The idealized simulations allowed for a mechanistic characterization of how phytoplankton community growth rates vary as a function of rate and magnitude of SST change (Sections 3.2 & 3.3). However, in the ocean, SST change is much more complicated as phytoplankton are exposed to a large variety of rates and durations of SST changes. We used Southern Ocean drifter trajectories to investigate the impact of *in situ* SST variability on community growth rates. When phenotypic diversity was considered (phenotype model), variable SST resulted in lower average community growth rates compared to the Eppley curve approximation (Figure 6). Though nutrient and light limitation were not explicitly included in the phenotype model, the simulated growth rates were consistent with *in situ* (Buitenhuis et al., 2013), remote-sensed based (Arteaga et al., 2020), and incubation derived growth rates (Boyd, 2019; Boyd et al., 2013), and therefore reasonably captured growth dynamics. As drifter SST variability increased, so did the difference between the phenotype model and the Eppley curve approximation, consistent with the idealized simulation results. The mean percent difference between the phenotype model and the Eppley curve approximation over the 90-day trajectories ranged between −142% and −11.5% with a mean of −25.8% (±16.6% 1σ) for the skewed reaction norms. A similar pattern was observed for the broad shaped reaction norms, but the magnitude of the difference was smaller and ranged from −53.2% to just −1.3% different with a mean of −6.1% (±5% 1σ) (Figure S20). Trajectories with higher mean SSTs were affected less by SST variability than trajectories with lower SSTs because faster growth rates at higher temperatures allowed quicker responses to SST changes.

To isolate the impact that short-term variability may have on community growth rates relative to longer-term shifts, we compared the 90-day mean biomass-weighted community growth rate of the drifter trajectories to the smoothed splines derived from the trajectories. Removing short-term variability had no significant impact on community growth rates (*t*-test, 95% CI; Figure S21).

4. Discussion

4.1. Impact of Acclimation

As ocean surface temperature shifts, two processes occur simultaneously: (a) individual phytoplankton phenotypes respond to the change in temperature (acclimation), and (b) phenotype abundance within the community shifts towards individuals with higher maximum growth rates at the new temperature. In this study, we investigated the impact of these individual-level dynamics on community-level growth. We demonstrate that shifts in phenotype abundance are the primary drivers of community growth rate dynamics. This is in large part due to *in situ* rates of SST changes being slower than the rates of individual acclimation (based on laboratory estimates), even for the dynamic Southern Ocean. When individual acclimation rates were slower than the rate of SST change, we observed a delay in the low growth phase and a smaller magnitude

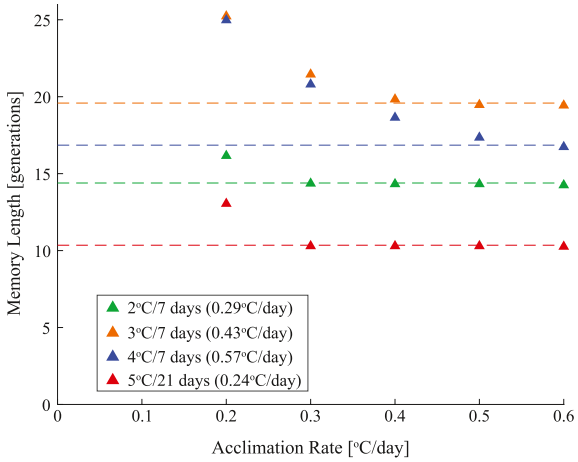

Figure 7. The impact of acclimation on the number of generations for which the effect of a temperature change persists (memory length). Acclimation rates that were slower than the rate of sea surface temperature (SST) change resulted in longer memory lengths than for simulations in which acclimation rate was equal to or faster than the SST rate of change.

decrease in community growth rates (Figure S22). The memory effect increased linearly as individual acclimation rates decreased (longer acclimation time) (Figures 7 and S23).

The representation of phenotype acclimation in the model was a simplistic representation of phenotypic plasticity (*see Methods*). In reality, plastic responses are much more complex and nonlinear and most likely vary among species (Kremer et al., 2018). Additional work is needed to better constrain both the range of acclimation timescales and the mechanisms of phenotypic plasticity. However, our results suggest that these dynamics will only become important under rapid temperature changes which are infrequent in the ocean.

4.2. Implications for In-Situ Community Composition

Our findings support the important role of thermal history in shaping the response of phytoplankton communities to changes in temperature. We have shown that SST variability can lower community growth rates for tens of generations following SST perturbation. This indicates that, for many regions of the ocean, the phytoplankton community will not be fully acclimated to local conditions as a result of the mismatch between timescales of physical variability and biological response. This mismatch in timescales will be a function of the rate and magnitude of SST variability that phytoplankton in the water mass were previously exposed to and may be reflected in physiological properties such as optimum growth temperature or overall community growth rate.

Our results also provide an important extension on the classic principle that "everything is everywhere: but the environment selects" (Hutchinson, 1961). Even when "everything is everywhere", we show that the timescale for environmental selection (community replacement) is a critical factor in determining community composition. Specifically, we hypothesize that even when the "optimal" organism is present in an environment, environmental variability generated by local physics, lateral advection, and seasonal trends can delay or prevent that organism from dominating the community. This hypothesis is supported by previous modeling work that has shown a time-lag on the order of weeks to a month in the phytoplankton community growth response to SST changes due to lateral advection and seasonal trends (Hellweger et al., 2016; Moisan, et al., 2002). Here, we have quantified the relationship between varying rates of SST variability and the timescale required for community replacement to impact the community composition.

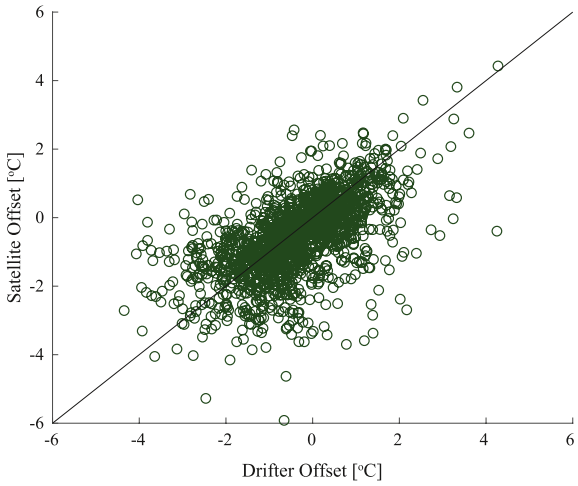

Figure 8. The impact of Lagrangian and Eulerian variability on community composition. Here we plot the difference between the T_{opt} of the most abundant phenotype at the end of each 90-day trajectory and the final sea surface temperature (SST) for the drifter trajectory (*x*-axis) and the satellite data (*y*-axis). The final SSTs for the drifter and satellite data are not statistically different (*t*-test, 95% CI). Therefore, deviations from the 1:1 line demonstrate the impact of a Lagrangian versus Eulerian reference frame on community composition.

We tested the impact of Eulerian versus Lagrangian variability on community growth rates and demonstrated significant differences for locations in which SST variability differed in the two reference frames. Specifically, while the final SST of the drifter segments and satellite data were not statistically different (*t*-test, 95% CI, Figure S24), differences in the nature of variability in the preceeding 90 days resulted in a significant difference between the final SST and the T_{opt} of the most abundant phenotype (*t*-test, 95% CI, Figures 8 and S25). The magnitude of the offset between SST and T_{opt} depended on the timing of SST changes throughout the 90-day profiles. When SST changes were slow, the offset between SST and the T_{opt} of the most abundant phenotype were negligible (Figure S26 for an example). Large SST changes that occurred early in the 90-day segment allowed sufficient time for the community to respond (e.g., Figure S26). When SST changes occurred later in the 90-days, the community did not have sufficient time to respond which caused a larger offset between the SST at day 90 and the T_{opt} of the community (e.g.,

Figure S27). Different phenotype distributions for the Eulerian versus Lagrangian reference frames is consistent with previous results that showed advection of phytoplankton communities was a key process in shaping phytoplankton diversity (Barton et al., 2010; Clayton et al., 2013; Lévy et al., 2014).

The shape of the reaction norm impacts the community response to temperature variability and phenotype competitive advantage. Under decreasing temperatures, a phenotype with a skewed reaction norm (T_{opt} closer to T_{max} than T_{min}) has a competitive advantage over a phenotype with a broad reaction norm (T_{opt} at the center of T_{max} and T_{min}), given the same reaction norm width and T_{opt}. A skewed reaction norm provides a larger range of temperatures $<T_{opt}$ under which the phenotype can grow. Therefore, organisms with skewed reaction norms should be adapted to have T_{opt} values close to maximum encountered temperatures not only due to the rapid decline in growth rates for temperatures greater than T_{opt} but also due to the competitive advantage under temperatures less than T_{opt}. Conversely, broad reaction norms are favored when temperatures are warming, as expected, or when temperatures are more variable. In a highly variable region such as the Southern Ocean, there should be selective pressure for either broad reaction norms with large growth ranges beyond T_{opt} (Moisan et al., 2002) or skewed reaction norms where T_{opt} is higher than mean SSTs (Thomas et al., 2012).

4.3. Implications for Simulating Community Growth Rates in Global Biogeochemical Models

A form of the Eppley curve, Q_{10} temperature-growth response ($\mu = \mu_0 Q_{10}^{\frac{T-T_0}{10}}$), is widely used in global biogeochemical models (Bopp et al., 2013), where typical model Q_{10} values range between 1.5 and 2 (Sherman et al., 2016). The premise behind employing a Q_{10} growth equation is that each modeled functional group encompasses many species or strains and so the Eppley curve may be a reasonable representation of the group dynamics. However, as we have demonstrated, community growth rates (or functional group growth rates in the model framework) will depend on the underlying phenotype dynamics, which are a function of the rate, magnitude, and direction of temperature change and the shape of the species/strains' thermal response curve. As a result, the Q_{10} temperature-growth response not only underestimates temperature-limitation on community growth rates (i.e., overestimates growth rates) but does so as a function of SST, SST variability, and reaction norm shape. Our work indicates that adjusting the Q_{10} relationship to use a lower exponent as previously suggested (Sherman et al., 2016) will only partially capture realistic dynamics. Because phytoplankton play a key role in sequestering carbon dioxide from the Earth's atmosphere, by overestimating phytoplankton growth rates, and thus overestimating carbon uptake, biogeochemical models may be underestimating the extent of future anthropogenic warming.

To predict changes in phytoplankton community growth rates robustly, models must also consider the impact of different types of SST variability and the appropriate reference frame for this variability. Specifically, we have shown that SST variability can differ markedly between the Eulerian reference frame and the Lagrangian reference frame (Figure S14). While the spatial patterns of SST variability in the Southern Ocean were similar between Eulerian and Lagrangian reference frames (Figures 9a–9c), the Eulerian reference frame exhibited substantially less variability. Consequentially, the offset between Eppley curve approximation and the phenotype model was substantially less for the Eulerian relative to the Lagrangian reference frame (Figures 9d–9f). This pattern was consistent for both the drifter Lagrangian trajectories and the satellite derived trajectories.

Models such as DARWIN (Follows et al., 2007) resolve phenotypes with a range of thermal reaction norms and so will capture the community growth rate dynamics presented here. However, additional work is needed to compare the variability encountered by functional group phenotypes in large-scale models integrated in an Eulerian framework to true Lagrangian variability.

Improving the parameterized temperature-growth relationship is particularly important in the Southern Ocean given the uncertainty of future primary productivity in this ocean basin (Bopp et al., 2013). We used our model results to identify key regions within the Southern Ocean that might be most strongly impacted by temperature variability. Three particular regions stand out that exhibited the most SST variability and had the largest relative deviations from the Eppley curve (Q_{10}) approximation: the Malvinas-Brazil confluence zone; the Agulhas Retroflection region; and downstream from these two along the Subtropical Front

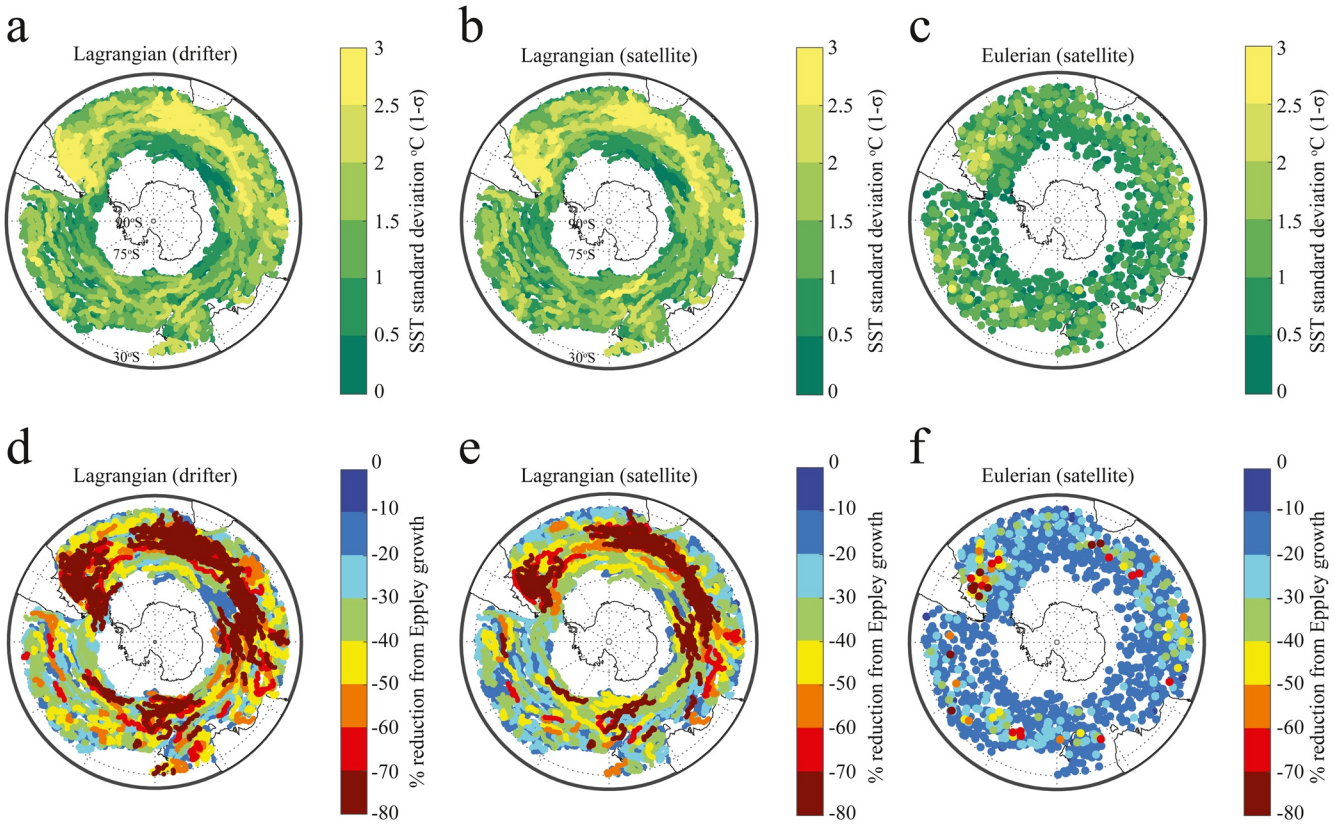

Figure 9. (a–c) Distribution of sea surface temperature (SST) variability and (d–f) the deviation in community growth rate from the Eppley growth model over the Southern Ocean (>30°S). Only those drifters which overlap in space and time with the satellite data are shown. For full results, see Figure S29. Three key regions of high SST variability stand out: Malvinas-Brazil confluence zone, the Agulhas Retroflection, and the Subtropical front. These regions have enhanced SST variability in all datasets but higher variability in the Lagrangian trajectories. These high variability regions correspond to large differences between the phenotype model growth rates and the Eppley approximation of growth, a pattern consistent across all three sets of simulations.

near ~45°S, 60°E (Figures 9a–9c). All three regions were previously identified as highly dynamic, strong frontal regions (Artana et al., 2019; Beal et al., 2015; Graham & Boer, 2013) and shown to be important hotspots for phytoplankton diversity (Barton et al., 2010; Clayton et al., 2013; d'Ovidio et al., 2010; Soccodato et al., 2016). It is possible that in these highly dynamic frontal regions the floats were subjected to physical movements across the fronts that was previously thought to elude phytoplankton movements. However, recent field and modeling studies have shown that cross-front transfer and diapycnal mixing can occur due to the fine-scale physics associated with these strong fronts (Clayton et al., 2017; Mahadevan, 2016; Wenegrat et al., 2020). Our results also showed that large SST changes were not required for temperature variations to have a lasting impact on community growth rates. Regions of the Southern Ocean with moderate (1–2°C, 1σ) SST variability also recorded equally large differences in community growth rate, often at least 30% smaller than Eppley curve approximations and up to 80% smaller than Eppley curve approximations.

5. Conclusions

We utilized idealized SST simulations and SST data from ocean surface drifters to show that synoptic SST variability on timescales of a few days to a few weeks decreases phytoplankton community growth rates, while higher frequency variability has little impact. The time taken for the community growth rate to reflect the new environment was dependent upon the rate and magnitude of temperature change, the direction of change, and the shape of the thermal response curve. The largest memory effects resulted from moderate changes in SST that occurred over 1–3 weeks. This impact of SST variability can cause a large offset between a phenotype-based temperature-dependent community growth rate and an Eppley curve-based approximation and suggests that phytoplankton communities sampled *in situ* may often not be adjusted to

local conditions. Given the highly variable nature of the ocean and importance of environmental variability for phytoplankton physiology, it is critical to consider the appropriate reference frame and the magnitude and duration of variability when studying phytoplankton dynamics. Here we demonstrate that variability captured in the Lagrangian reference frame (by drifters) was, in many instances, different from variability in the Eulerian frame and that this had significant impacts for estimating phytoplankton growth rates. These findings have potentially far-reaching implications for how temperature-dependent phytoplankton growth is represented in global biogeochemical models.

Data Availability Statement

Drifter data used here can be obtained from the Drifter Data Centre at the Atlantic Oceanographic and Meteorological Laboratory (https://www.aoml.noaa.gov/phod/gdp/) and satellite data are available from the GHRSST Level 4 MUR Global Foundation Sea Surface Temperature Analysis (https://podaac.jpl.nasa.gov/dataset/MUR-JPL-L4-GLOB-v4.1).

Acknowledgments
We would like to thank Robert Strzepek for providing us with the acclimation rate data (Table S2) and anonymous reviewers for their constructive feedback. Additionally, we acknowledge funding support from the National Science Foundation (NSF OCE 1538525 to N. M. Levine). P. W. Boyd was supported by an ARC Laureate fellowship and the Australian Department of Industry funded Australian Antarctic Program Partnership. S. C. Doney acknowledges support from NSF Office of Polar Programs (grant PLR-1440435 to the Palmer Long Term Ecological Research project). J. N. Havenhand acknowledges support from the University of Gothenburg Natural Sciences Sabbatical Program.

References

Artana, C., Provost, C., Lellouche, J., Rio, M., Ferrari, R., & Sennéchael, N. (2019). The Malvinas current at the Confluence with the Brazil current: Inferences from 25 years of Mercator Ocean reanalysis. *Journal of Geophysical Research: Oceans*, *124*(10), 7178–7200. https://doi.org/10.1029/2019JC015289

Arteaga, L. A., Boss, E., Behrenfeld, M. J., Westberry, T. K., & Sarmiento, J. L. (2020). Seasonal modulation of phytoplankton biomass in the Southern Ocean. *Nature Communications*, *11*(1), 5364. https://doi.org/10.1038/s41467-020-19157-2

Barton, A. D., Dutkiewicz, S., Flierl, G., Bragg, J., & Follows, M. J. (2010). Patterns of diversity in marine phytoplankton. *Science*, *327*(5972), 1509–1511. https://doi.org/10.1126/science.1184961

Beal, L. M., Elipot, S., Houk, A., & Leber, G. M. (2015). Capturing the transport variability of a western boundary jet: Results from the Agulhas Current Time-Series Experiment (ACT). *Journal of Physical Oceanography*, *45*(5), 1302–1324. https://doi.org/10.1175/JPO-D-14-0119.1

Bernhardt, J. R., Sunday, J. M., Thompson, P. L., & O'Connor, M. I. (2018). Nonlinear averaging of thermal experience predicts population growth rates in a thermally variable environment. *Proceedings of the Royal Society B: Biological Sciences*, *285*, 20181076. https://doi.org/10.1098/rspb.2018.1076

Bopp, L., Resplandy, L., Orr, J. C., Doney, S. C., Dunne, J. P., Gehlen, M., et al. (2013). Multiple stressors of ocean ecosystems in the 21st century: Projections with CMIP5 models. *Biogeosciences*, *10*(10), 6225–6245. https://doi.org/10.5194/bg-10-6225-2013

Boyd, P. W. (2019). Physiology and iron modulate diverse responses of diatoms to a warming Southern Ocean. *Nature Climate Change*, *9*(2), 148–152. https://doi.org/10.1038/s41558-018-0389-1

Boyd, P. W., Cornwall, C. E., Davison, A., Doney, S. C., Fourquez, M., Hurd, C. L., et al. (2016). Biological responses to environmental heterogeneity under future ocean conditions. *Global Change Biology*, *22*(8), 2633–2650. https://doi.org/10.1111/gcb.13287

Boyd, P. W., Rynearson, T. A., Armstrong, E. A., Fu, F., Hayashi, K., Hu, Z., et al. (2013). Marine phytoplankton temperature versus growth responses from polar to tropical waters – Outcome of a scientific community-wide study. *PloS One*, *8*(5), e63091. https://doi.org/10.1371/journal.pone.0063091

Buitenhuis, E. T., Hashioka, T., & Quéré, C. L. (2013). Combined constraints on global ocean primary production using observations and models. *Global Biogeochemical Cycles*, *27*(3), 847–858. https://doi.org/10.1002/gbc.20074

Clayton, S., Dutkiewicz, S., Jahn, O., & Follows, M. J. (2013). Dispersal, eddies, and the diversity of marine phytoplankton. *Limnology and Oceanography: Fluids and Environments*, *3*(1), 182–197. https://doi.org/10.1215/21573689-2373515

Clayton, S., Lin, Y.-C., Follows, M. J., & Worden, A. Z. (2017). Co-existence of distinct Ostreococcus ecotypes at an oceanic front. *Limnology and Oceanography*, *62*(1), 75–88. https://doi.org/10.1002/lno.10373

Cochlan, W. (2008). *Nitrogen uptake in the Southern Ocean* (pp. 569–596). https://doi.org/10.1016/b978-0-12-372522-6.00012-8

Deser, C., Alexander, M. A., Xie, S.-P., & Phillips, A. S. (2010). Sea surface temperature variability: Patterns and mechanisms. *Annual Review of Marine Science*, *2*(1), 115–143. https://doi.org/10.1146/annurev-marine-120408-151453

Doblin, M. A., & van Sebille, E. (2016). Drift in ocean currents impacts intergenerational microbial exposure to temperature. *Proceedings of the National Academy of Sciences of the United States of America*, *113*(20), 5700–5705. https://doi.org/10.1073/pnas.1521093113

Doney, S. C. (1999). Major challenges confronting marine biogeochemical modeling. *Global Biogeochemical Cycles*, *13*(3), 705–714. https://doi.org/10.1029/1999GB900039

d'Ovidio, F., De Monte, S., Alvain, S., Dandonneau, Y., & Levy, M. (2010). Fluid dynamical niches of phytoplankton types. *Proceedings of the National Academy of Sciences of the United States of America*, *107*(43), 18366–18370. https://doi.org/10.1073/pnas.1004620107

Eppley, R. (1972). Temperature and phytoplankton growth in the sea. *Fishery Bulletin*, *70*(4), 1063–1085.

Falkowski, P. G., Fenchel, T., & Delong, E. F. (2008). The microbial engines that drive Earth's biogeochemical cycles. *Science*, *320*(5879), 1034–1039. https://doi.org/10.1126/science.1153213

Follows, M. J., Dutkiewicz, S., Grant, S., & Chisholm, S. W. (2007). Emergent biogeography of microbial communities in a model ocean. *Science*, *315*(5820), 1843–1846. https://doi.org/10.1126/science.1138544

Fu, W., Randerson, J. T., & Moore, J. K. (2016). Climate change impacts on net primary production (NPP) and export production (EP) regulated by increasing stratification and phytoplankton community structure in the CMIP5 models. *Biogeosciences*, *13*(18), 5151–5170. https://doi.org/10.5194/bg-13-5151-2016

Graham, R. M., & Boer, A. M. D. (2013). The dynamical subtropical front. *Journal of Geophysical Research: Oceans*, *118*(10), 5676–5685. https://doi.org/10.1002/jgrc.20408

Hellweger, F. L., van Sebille, E., Calfee, B. C., Chandler, J. W., Zinser, E. R., Swan, B. K., & Fredrick, N. D. (2016). The role of ocean currents in the temperature selection of plankton: Insights from an individual-based model. *PloS One*, *11*(12), e0167010. https://doi.org/10.1371/journal.pone.0167010

Hutchinson, G. E. (1961). The paradox of the plankton. *The American Naturalist*, *95*(882), 137–145. https://doi.org/10.1086/282171

Kling, J. D., Lee, M. D., Fu, F., Phan, M. D., Wang, X., Qu, P., & Hutchins, D. A. (2019). Transient exposure to novel high temperatures reshapes coastal phytoplankton communities. *The ISME Journal*, *14*, 413–424. https://doi.org/10.1038/s41396-019-0525-6

Kremer, C. T., Fey, S. B., Arellano, A. A., & Vasseur, D. A. (2018). Gradual plasticity alters population dynamics in variable environments: Thermal acclimation in the green alga *Chlamydomonas reinhartdii*. *Proceedings of the Royal Society B: Biological Sciences*, *285*(1870), 20171942. https://doi.org/10.1098/rspb.2017.1942

Laufkötter, C., Vogt, M., Gruber, N., Aita-Noguchi, M., Aumont, O., Bopp, L., et al. (2015). Drivers and uncertainties of future global marine primary production in marine ecosystem models. *Biogeosciences*, *12*(23), 6955–6984. https://doi.org/10.5194/bg-12-6955-2015

Lévy, M., Jahn, O., Dutkiewicz, S., & Follows, M. J. (2014). Phytoplankton diversity and community structure affected by oceanic dispersal and mesoscale turbulence. *Limnology and Oceanography: Fluids and Environments*, *4*(1), 67–84. https://doi.org/10.1215/21573689-2768549

Lomas, M. W., Steinberg, D. K., Dickey, T., Carlson, C. A., Nelson, N. B., Condon, R. H., & Bates, N. R. (2010). Increased ocean carbon export in the Sargasso Sea linked to climate variability is countered by its enhanced mesopelagic attenuation. *Biogeosciences*, *7*(1), 57–70. https://doi.org/10.5194/bg-7-57-2010

Mahadevan, A. (2016). The impact of submesoscale physics on primary productivity of plankton. *Annual Review of Marine Science*, *8*(1), 161–184. https://doi.org/10.1146/annurev-marine-010814-015912

Maheshwari, M., Singh, R. K., Oza, S. R., & Kumar, R. (2013). An investigation of the Southern Ocean surface temperature variability using long-term optimum interpolation SST data. *ISRN Oceanography*, *2013*, 1–9. https://doi.org/10.5402/2013/392632

Moisan, J. R., Moisan, T. A., & Abbott, M. R. (2002). Modelling the effect of temperature on the maximum growth rates of phytoplankton populations. *Ecological Modelling*, *153*(3), 197–215. https://doi.org/10.1016/S0304-3800(02)00008-X

Qu, P., Fu, F.-X., Kling, J. D., Huh, M., Wang, X., & Hutchins, D. A. (2019). Distinct responses of the nitrogen-fixing marine Cyanobacterium Trichodesmium to a thermally variable environment as a function of phosphorus availability. *Frontiers in Microbiology*, *10*, 1282. https://doi.org/10.3389/fmicb.2019.01282

Quéré, C. L., Harrison, S. P., Prentice, I. C., Buitenhuis, E. T., Aumont, O., Bopp, L., et al. (2005). Ecosystem dynamics based on plankton functional types for global ocean biogeochemistry models. *Global Change Biology*, *11*(11), 2016–2040. https://doi.org/10.1111/j.1365-2486.2005.1004.x

Reynolds, R. W., & Smith, T. M. (1994). Improved global sea surface temperature analyses using optimum interpolation. *Journal of Climate*, *7*(6), 929–948. https://doi.org/10.1175/1520-0442(1994)007<0929:IGSSTA>2.0.CO;2

Rohr, T., Harrison, C., Long, M. C., Gaube, P., & Doney, S. C. (2020a). Eddy-modified iron, light, and phytoplankton cell division rates in the simulated Southern Ocean. *Global Biogeochemical Cycles*, *34*(6), e2019GB006380. https://doi.org/10.1029/2019GB006380

Rohr, T., Harrison, C., Long, M. C., Gaube, P., & Doney, S. C. (2020b). The simulated biological response to Southern Ocean eddies via biological rate modification and physical transport. *Global Biogeochemical Cycles*, *34*(6), e2019GB006385. https://doi.org/10.1029/2019GB006385

Schaum, C.-E., Buckling, A., Smirnoff, N., Studholme, D. J., & Yvon-Durocher, G. (2018). Environmental fluctuations accelerate molecular evolution of thermal tolerance in a marine diatom. *Nature Communications*, *9*(1), 1719. https://doi.org/10.1038/s41467-018-03906-5

Sherman, E., Moore, J. K., Primeau, F., & Tanouye, D. (2016). Temperature influence on phytoplankton community growth rates. *Global Biogeochemical Cycles*, *30*(4), 550–559. https://doi.org/10.1002/2015GB005272

Soccodato, A., d'Ovidio, F., Lévy, M., Jahn, O., Follows, M. J., & De Monte, S. (2016). Estimating planktonic diversity through spatial dominance patterns in a model ocean. *Marine Genomics*, *29*, 9–17. https://doi.org/10.1016/j.margen.2016.04.015

Thomas, M. K., Kremer, C. T., Klausmeier, C. A., & Litchman, E. (2012). A global pattern of thermal adaptation in marine phytoplankton. *Science*, *338*(6110), 1085–1088. https://doi.org/10.1126/science.1224836

Wang, X., Fu, F., Qu, P., Kling, J. D., Jiang, H., Gao, Y., & Hutchins, D. A. (2019). How will the key marine calcifier Emiliania huxleyi respond to a warmer and more thermally variable ocean? *Biogeosciences*, *16*(22), 4393–4409. https://doi.org/10.5194/bg-16-4393-2019

Webb, E. A., Ehrenreich, I. M., Brown, S. L., Valois, F. W., & Waterbury, J. B. (2009). Phenotypic and genotypic characterization of multiple strains of the diazotrophic cyanobacterium, Crocosphaera watsonii, isolated from the open ocean. *Environmental Microbiology*, *11*(2), 338–348. https://doi.org/10.1111/j.1462-2920.2008.01771.x

Wenegrat, J. O., Thomas, L. N., Sundermeyer, M. A., Taylor, J. R., D'Asaro, E. A., Klymak, J. M., et al. (2020). Enhanced mixing across the gyre boundary at the Gulf Stream front. *Proceedings of the National Academy of Sciences of the United States of America*, *117*, 17607–17614. https://doi.org/10.1073/pnas.2005558117